

This document contains a post-print version of the paper

Nonlinear pressure control of self-supplied variable displacement axial piston pumps

authored by **W. Kemmetmüller, F. Fuchshumer, and A. Kugi**
and published in *Control Engineering Practice*.

The content of this post-print version is identical to the published paper but without the publisher's final layout or copy editing. Please, scroll down for the article.

Cite this article as:

W. Kemmetmüller, F. Fuchshumer, and A. Kugi, "Nonlinear pressure control of self-supplied variable displacement axial piston pumps", *Control Engineering Practice*, vol. 18, pp. 84–93, 2010. DOI: [10.1016/j.conengprac.2009.09.006](https://doi.org/10.1016/j.conengprac.2009.09.006)

BibTex entry:

```
% This file was created with JabRef 2.9.2.  
% Encoding: Cp1252  
  
@ARTICLE{acinpaper,  
  author = {Kemmetmüller, W. and Fuchshumer, F. and Kugi, A.},  
  title = {Nonlinear pressure control of self-supplied variable displacement  
          axial piston pumps},  
  journal = {Control Engineering Practice},  
  year = {2010},  
  volume = {18},  
  pages = {84-93},  
  doi = {10.1016/j.conengprac.2009.09.006},  
  url = {http://www.sciencedirect.com/science/article/pii/S0967066109001701}  
}
```

Link to original paper:

<http://dx.doi.org/10.1016/j.conengprac.2009.09.006>
<http://www.sciencedirect.com/science/article/pii/S0967066109001701>

Read more ACIN papers or get this document:

<http://www.acin.tuwien.ac.at/literature>

Contact:

Automation and Control Institute (ACIN)
Vienna University of Technology
Gusshausstrasse 27-29/E376
1040 Vienna, Austria

Internet: www.acin.tuwien.ac.at
E-mail: office@acin.tuwien.ac.at
Phone: +43 1 58801 37601
Fax: +43 1 58801 37699

Copyright notice:

This is the authors' version of a work that was accepted for publication in *Control Engineering Practice*. Changes resulting from the publishing process, such as peer review, editing, corrections, structural formatting, and other quality control mechanisms may not be reflected in this document. Changes may have been made to this work since it was submitted for publication. A definitive version was subsequently published in W. Kemmetmüller, F. Fuchshumer, and A. Kugi, "Nonlinear pressure control of self-supplied variable displacement axial piston pumps", *Control Engineering Practice*, vol. 18, pp. 84–93, 2010. DOI: [10.1016/j.conengprac.2009.09.006](https://doi.org/10.1016/j.conengprac.2009.09.006)

Nonlinear pressure control of self-supplied variable displacement axial piston pumps

W. Kemmetmüller^{*a}, F. Fuchshumer^b, A. Kugi^a

^aAutomation and Control Institute, Vienna University of Technology, Gusshausstr. 27–29, 1040 Vienna, Austria

^bHydac Electronic GmbH, Hauptstr. 27, 66128 Saarbrücken, Germany

Abstract

The present paper deals with the pressure control of self-supplied variable displacement axial piston pumps subject to fast changing, unknown loads. First, the setup of the system and the mathematical model are described. As the pump is self-supplied, the mathematical model exhibits a switching right-hand side which makes the control design a challenging task. A nonlinear two degrees-of-freedom control strategy, comprising a feedforward and a feedback control, in combination with a load estimator is proposed for the pressure control. The proof of the stability of the overall closed-loop system is based on Lyapunov's theory. The performance of the control concept is verified by means of experiments. The results show that the proposed control concept has an excellent and robust behavior.

Key words: axial piston pumps, nonlinear control, switched systems, load estimation, load-sensing, pressure control

1. Introduction

Electrohydraulic systems are widely spread in many industrial plants and mobile machines like excavators, cranes, etc., which is mainly due to the very high power density of hydraulic systems compared to electrical or mechanical drives. The generally poor energetic efficiency constitutes one of the major drawbacks of electrohydraulic systems. Conventional hydraulic supply systems typically provide a constant supply pressure or a constant supply volume flow, independent of the actual demands of the load. Thus, the worst energetic efficiency occurs in the case when no energy is needed by the load. The increasing demands on the energetic efficiency requires the implementation of hydraulic supply systems which can be adjusted to the actual requirements of the load (load-sensing), see, e.g., Wu, Burton, Schoenau & Bitner (2002); Findeisen (2006). Basically, two approaches do exist to control the supply volume flow.

If a fixed displacement pump is used, then the input speed of the pump can be utilized to change the output volume flow. In many applications, fixed displacement pumps are driven by electric motors which allow an easy control of the speed. The dynamics, however, are very limited such that in general the demands on the dynamical performance cannot be met with this concept. This is even more obvious if the pump is driven by a combustion engine.

The second possibility to control the volume flow of a pump is to change the displacement of the pump. In this context, variable-displacement axial piston pumps are often used, whereby the displacement of the pump (i.e. the volume flow)

can be changed by tilting a swash plate. This can be done fast enough to meet the dynamical demands of many loads.

The present paper deals with the supply pressure control of electrohydraulic systems comprising a variable displacement axial piston pump and a variable load. Typically, linear control strategies are used in such applications, see, e.g., Grabbel & Ivantysynova (2005); Wu, Burton, Schoenau & Bitner (2002). Since electrohydraulic systems exhibit a significant nonlinear behavior the performance of the closed-loop system is normally rather limited. Furthermore, a rigorous stability proof is lacking in most cases and the tuning of the controller parameters turns out to be very time-consuming. In this work, a new model-based nonlinear control strategy is derived, which, on the one hand, takes into account the essential nonlinearities of the system and, on the other hand, can be easily adjusted to pumps of different installation sizes in the same model range.

A general problem in designing a load-sensing system is to find out the actual demands of the load, since in most cases the load is neither known nor can it be measured. This problem also occurs in the application considered in this paper where the load not only is unknown but may also change in a very fast manner. In order to deal with this fact, the nonlinear control strategy has to be augmented by a load estimator. This is a challenging task since it is well known that the separation principle of the controller and the estimator design does not hold for nonlinear systems. In this contribution, the stability of the closed-loop system consisting of the nonlinear controller, the nonlinear load estimator and the plant model is proven by means of Lyapunov's theory.

In order to meet the high demands both on the tracking behavior and the robustness of the closed-loop system a two degrees-of-freedom control structure, comprising a feedforward and a feedback part, is proposed in the controller design. Thereby, the design of the control strategy becomes very chal-

*Corresponding Author: Tel./Fax: +43(0)1 58801-77625/-37699

Email addresses: kemmetmuller@acin.tuwien.ac.at (W. Kemmetmüller), franz.fuchshumer@hydac.com (F. Fuchshumer), kugi@acin.tuwien.ac.at (A. Kugi)

lenging in the considered application due to the fact that the axial piston pump is self-supplied, i.e. the volume flow which is necessary to control the pump is taken from the output volume flow of the pump. This, as will be outlined in detail in the next section, yields a switching mathematical model of the system. It is well known from literature that the controller design and the proof of the stability is much more demanding for switching systems (Branicky, 1995, 1998; DeCarlo, Branicky, Pettersson & Lennartson, 2000; Liberzon, 2003).

The paper is organized as follows: In the next section, the electrohydraulic system under consideration is described in detail and a short overview of the mathematical modeling as well as a precise definition of the control task is given. Section 3 is concerned with the control design, whereby a feedforward controller is designed in the first part and is augmented by a feedback controller in the second part. The design of a load estimator is the topic of Section 4, where a simple and an extended estimator for the load is presented. Finally, the feasibility of the overall control concept is shown by means of measurement results in Section 5.

2. Mathematical Modeling and Control Task

The variable displacement axial piston pump under consideration is to be used in injection molding machines, where liquid plastics is injected into a mold by a screw conveyor. The displacement of the screw conveyor is controlled by a hydraulic piston actuator, which, in turn, is controlled by the axial piston pump. Basically, the injection process can be divided into two phases:

- i. In the first phase, the mold is filled with liquid plastics. To accomplish this task, the screw conveyor has to be moved with a constant velocity. This means that the axial piston pump has to provide a constant volume flow.
- ii. In the second phase, the mold is completely filled. In order to compensate for the shrinking of the cooling plastics, liquid plastics has to be supplied to the mold with constant pressure. Thus, the axial piston pump has to control the pressure in the piston actuator.

The control task for the first phase is rather simple since the volume flow q_p of the pump is basically proportional to the swash plate angle φ_p . Thus, a simple (linear) controller for the swash plate angle turns out to be sufficient in terms of accuracy and dynamic performance, see, e.g., Fuchshumer (2009). On the other hand, the control of the pressure in the piston actuator is a challenging task since (i) there are very high demands on the dynamics and the accuracy of the pressure and (ii) the characteristics of the load can change dramatically with very high dynamics. The control task is further complicated by the fact that the pump is self-supplied, which means that the volume flow necessary to control the swash plate angle of the pump is taken from the pump volume flow q_p , cf. Fig. 2. This in turn entails a switching character of the mathematical model.

In Fig. 1 the schematic diagram of a variable displacement axial piston pump is shown. The pump under consideration

consists of 9 pistons which are placed in the barrel. The barrel, driven by an induction machine, rotates with the (almost constant) angular velocity ω_p and is forced against the valve plate, which alternately connects the pistons to the tank and to the load pressure. The pistons themselves are born against the swash plate by means of slippers. A tilt (angle φ_p) of the swash plate results in an axial displacement of the pistons. Thereby, oil is taken from the tank via the intake port and delivered to the load via the discharge port. The volume flow of the pump q_p can be changed continuously by changing φ_p .

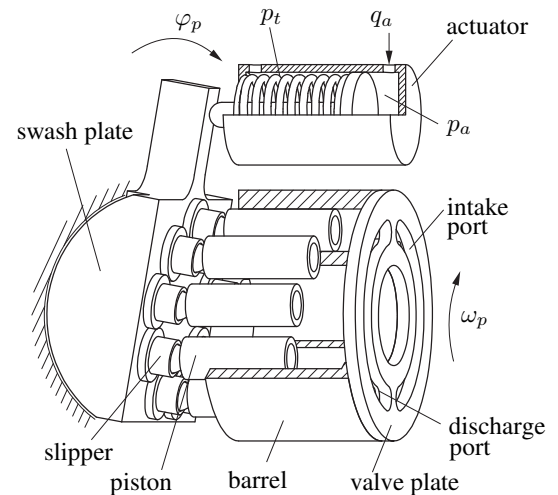


Figure 1: Schematic diagram of the variable displacement axial piston pump.

Fig. 2 depicts the schematic diagram of the overall electrohydraulic system under consideration. It comprises the variable displacement pump which delivers the volume flow q_p to the load volume V_l . The load volume is connected to the tank with tank pressure p_t via a variable load orifice. In order to change the volume flow q_p of the pump, the angle φ_p of the swash plate has to be adjusted. For this task a single acting hydraulic actuator is used, whereby the restoring force is generated by a spring. The actuator pressure p_a is controlled by a 3 ways / 3 lands (3/3) proportional directional valve generating the actuator volume flow q_a . As shown in Fig. 2, the control valve is supplied by the load pressure p_l , i.e., the pump is self-supplied. Thereby, only positive actuator volume flows q_a are taken from the load, while negative volume flows are discharged to the tank. The advantage of the chosen experimental setup is that all relevant situations occurring in injection moulding machines can be emulated under well-defined conditions.

The mathematical modeling of electrohydraulic systems was the topic of numerous works, see, e.g., Blackburn, Reethof & Shearer (1960), Merritt (1967) and McCloy & Martin (1980) for a general overview. Especially, detailed works are available for the mathematical modeling of variable displacement pumps (Manring & Johnson, 1996; Manring, 2005; Ivantysyn J & Ivantysynova M, 1993; Findeisen, 2006). Since the detailed mathematical models capturing all the dynamical effects are in general rather complicated they are not suitable for a model

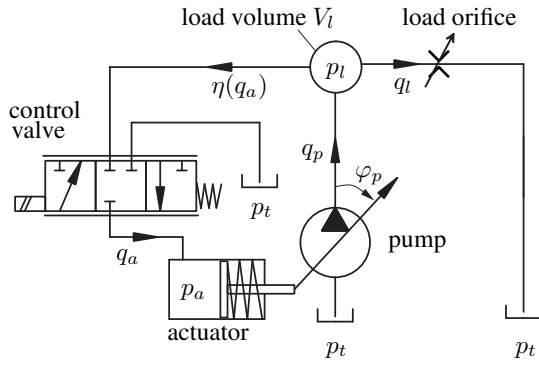


Figure 2: Schematic diagram of the electrohydraulic system.

based controller design. Therefore, an analysis of the dynamics of the system based on the singular perturbation theory was performed in Fuchshumer (2009) to systematically reduce the overall complexity of the mathematical model. The resulting model, which will be used in the subsequent control design, is given by

$$\frac{d}{dt}\varphi_p = -\frac{q_a}{A_a r_a} \quad (1a)$$

$$\frac{d}{dt}p_l = \frac{\beta}{V_l} (k_p \varphi_p - k_l \sqrt{p_l} - \eta(q_a)), \quad (1b)$$

where φ_p is the swash plate angle, p_l is the load pressure and q_a is the volume flow into the actuator. The effective area of the actuator is denoted by A_a and the effective radius is given by r_a . Further, β is the bulk modulus of the oil, V_l is the volume of the load and k_l denotes the unknown coefficient of the load orifice (load coefficient). The function $\eta(q_a)$ describes the volume flow taken from the load in order to tilt the swash plate

$$\eta(q_a) = \begin{cases} q_a & \text{for } q_a > 0 \\ 0 & \text{else.} \end{cases} \quad (2)$$

Finally, the volume flow q_p of the pump is given by $q_p = k_p \varphi_p$ with the pump coefficient

$$k_p = \frac{n_p A_p r_p \omega_p}{\pi}, \quad (3)$$

with the number of pistons n_p , the cross-sectional area A_p of a piston, the effective radius of rotation r_p of the pistons and the constant angular velocity ω_p of the barrel. As was shown in Fuchshumer (2009), this considerably simplified mathematical model of the electrohydraulic system in Fig. 2 covers the essential (nonlinear) behavior of the real system and thus serves as a good basis for the controller design.

Remark 1. Henceforth it is assumed that the volume flow q_a into the actuator is the control input of the system. In reality, of course, only the position of the spool of the 3/3 proportional directional valve can be directly controlled. However, a servo-compensation is implemented in the system which calculates the spool position s_v necessary to achieve a desired actuator volume flow q_a . More details on this topic will be given in Section 5.

The control design task can now be summarized as follows: Given the (nonlinear) mathematical model of the system (1), (2), design a (nonlinear) controller (with q_a as the control input) for the load pressure p_l which is capable of following high dynamic trajectories $p_{l,d}(t)$ without exact knowledge of the load. The control task is complicated by the following facts:

- From (1), (2) it can be seen that the mathematical model of the electrohydraulic system constitutes a switching system, since the right-hand side is changing dependent on the sign of q_a . This means, of course, that many classical stability results and control design methods for nonlinear systems cannot be directly applied.
- In addition to the fact that the load coefficient k_l is unknown in the real application, it can even change very rapidly.
- The controller has to be robust with respect to model uncertainties and measurement noise.

3. Control Design

This section is concerned with the development of a nonlinear model based control strategy for the electrohydraulic system (1), (2). In this work, a two degrees-of-freedom control structure comprising a feedforward and a feedback part is used to solve the aforementioned control task. In order to take into account the unknown load coefficient k_l , the controller is augmented by an estimator for k_l .

For the subsequent considerations, system (1), (2) is formally split into two systems: system Σ^I which is valid for $q_a \leq 0$,

$$\Sigma^I : \frac{d}{dt}\varphi_p = -\frac{q_a}{A_a r_a} \quad (4a)$$

$$\frac{d}{dt}p_l = \frac{\beta}{V_l} (k_p \varphi_p - k_l \sqrt{p_l}), \quad (4b)$$

and system Σ^{II} which holds for $q_a > 0$

$$\Sigma^{II} : \frac{d}{dt}\varphi_p = -\frac{q_a}{A_a r_a} \quad (5a)$$

$$\frac{d}{dt}p_l = \frac{\beta}{V_l} (k_p \varphi_p - k_l \sqrt{p_l} - q_a). \quad (5b)$$

3.1. Feedforward Control

System Σ^I

A simple investigation of (4) shows that the system Σ^I is differentially flat with the load pressure p_l as a possible flat output, see, e.g., Fliess, Lévine, Martin & Rouchon (1995) for an introduction to the concept of flatness for nonlinear systems. Defining a sufficiently smooth (at least twice continuously differentiable) desired trajectory $p_{l,d}$ of the load pressure in (4b) yields

$$\dot{p}_{l,d} = \frac{\beta}{V_l} (k_p \varphi_{p,d} - k_l \sqrt{p_{l,d}}). \quad (6)$$

In order to calculate the desired swash plate angle $\varphi_{p,d}$ from (6) the knowledge of the load coefficient k_l would be necessary. To circumvent this problem at this point, an estimation \hat{k}_l is used in the feedforward control instead of k_l . The design of the estimator and the proof of the overall closed-loop stability will be treated later on in this paper. For the time being only the existence of an appropriate estimator for k_l is presumed. This directly gives the desired swash plate angle $\varphi_{p,d}$

$$\varphi_{p,d} = \frac{1}{k_p} \left(\frac{V_l}{\beta} \dot{p}_{l,d} + \hat{k}_l \sqrt{p_{l,d}} \right). \quad (7)$$

The second derivative of the desired load pressure

$$\ddot{p}_{l,d} = \frac{\beta}{V_l} \left(-\frac{k_p}{A_a r_a} q_{a,d} - \frac{1}{2} \frac{\hat{k}_l}{\sqrt{p_{l,d}}} \dot{p}_{l,d} - \hat{k}_l \sqrt{p_{l,d}} \right) \quad (8)$$

includes the desired actuator volume flow $q_{a,d}$. Thus, the feedforward control¹ for Σ^I reads as

$$FF^I : \quad q_{a,d} = -\frac{A_a r_a}{k_p} \left(\frac{V_l}{\beta} \ddot{p}_{l,d} + \frac{1}{2} \frac{\hat{k}_l}{\sqrt{p_{l,d}}} \dot{p}_{l,d} + \hat{k}_l \sqrt{p_{l,d}} \right). \quad (9)$$

System Σ^{II}

In contrast to Σ^I , the load pressure p_l is no longer a flat output for Σ^{II} . Nevertheless, an inversion-based feedforward control strategy can be applied to this system. Thus, the desired load pressure $p_{l,d}$ is used in (5b)

$$\dot{p}_{l,d} = \frac{\beta}{V_l} (k_p \varphi_{p,d} - k_l \sqrt{p_{l,d}} - q_{a,d}), \quad (10)$$

yielding the desired volume flow $q_{a,d}$ for Σ^{II} with k_l replaced by \hat{k}_l in the form

$$FF^{II} : \quad q_{a,d} = -\frac{V_l}{\beta} \dot{p}_{l,d} + k_p \varphi_{p,d} - \hat{k}_l \sqrt{p_{l,d}}. \quad (11)$$

The corresponding desired swash plate angle $\varphi_{p,d}$ in (11) is determined by the differential equation for the internal dynamics

$$\frac{d}{dt} \varphi_{p,d} = \frac{1}{A_a r_a} \left(-k_p \varphi_{p,d} + \hat{k}_l \sqrt{p_{l,d}} + \frac{V_l}{\beta} \dot{p}_{l,d} \right). \quad (12)$$

Obviously, the internal dynamics is exponentially stable.

3.2. Feedback Control

The feedforward control designed in the last subsection has to be augmented by a feedback control in order to stabilize the tracking error in case of parameter variations or model uncertainties. Therefore, the pressure error $e_p = p_l - p_{l,d}$ and the error in the swash plate angle $e_\varphi = \varphi_p - \varphi_{p,d}$ are introduced. Applying FF^I to the system Σ^I yields the error system for $q_a \leq 0$

$$\frac{d}{dt} e_\varphi = -\frac{1}{A_a r_a} q_{a,c} \quad (13a)$$

$$\frac{d}{dt} e_p = \frac{\beta}{V_l} (k_p e_\varphi - k_l \sqrt{e_p + p_{l,d}} + \hat{k}_l \sqrt{p_{l,d}}), \quad (13b)$$

¹Subsequently, the feedforward control for Σ^I and Σ^{II} will be referred to by FF^I and FF^{II} , respectively.

where $q_{a,c} = q_a - q_{a,d}$ denotes the feedback part of the control input. Similarly for $q_a > 0$, using FF^{II} in Σ^{II} results in

$$\frac{d}{dt} e_\varphi = -\frac{1}{A_a r_a} q_{a,c} \quad (14a)$$

$$\frac{d}{dt} e_p = \frac{\beta}{V_l} (k_p e_\varphi - k_l \sqrt{e_p + p_{l,d}} + \hat{k}_l \sqrt{p_{l,d}} - q_{a,c}). \quad (14b)$$

Before a controller can be designed for the switched system (13), (14), some important facts on the stability of switched systems have to be discussed. First of all, it is well known from literature that a switched system may be unstable even if the individual systems are all stable for themselves (Branicky, 1995, 1998; DeCarlo, Branicky, Pettersson & Lennartson, 2000; Liberzon, 2003). Therefore, it is not sufficient to design a stabilizing controller for the error systems (13) and (14) separately. One possibility to achieve a systematic proof of the stability of switched systems is given by the method of multiple Lyapunov functions as proposed by Branicky (1998). Thereby, the stability of each system has to be proven with a Lyapunov function and in addition it has to be shown that each Lyapunov function is strictly non-increasing during switching. While the proof of the first condition is rather straightforward for many systems, the proof of the second condition is in general difficult. One way to avoid the proof of the second condition is to use a common Lyapunov function for all systems. Although the design of a common Lyapunov function turns out to be a rather delicate issue for general nonlinear switching systems, this approach will be pursued in the following.

For the time being, it is assumed that a common Lyapunov function and feedback controllers FB^I and FB^{II} for the error systems I and II , respectively, have already been found such that the stability of each closed-loop system is guaranteed². At this point the question arises when and how the control law consisting of the feedforward and the feedback control is switched. The intuitive approach would be that $FF^I + FB^I$ are active for $q_a \leq 0$ and $FF^{II} + FB^{II}$ for $q_a > 0$.

Then, however, two problems occur: First, switching the feedforward control FF^I and FF^{II} based on $q_a = 0$ yields to discontinuities in the desired value of the swash plate angle $\varphi_{p,d}$ and thus in e_φ . In order to make this more obvious, consider at the beginning that $q_a = q_{a,d} + q_{a,c} < 0$ and therefore FF^I and FB^I are active. If at time t_s the volume flow q_a equals zero, switching to FF^{II} and FB^{II} would occur. In this case, the initial value $\varphi_{p,d}(t_s)$ of the differential equation (12) would be set to the actual value of $\varphi_{p,d}$ at $t = t_s$ in FF^I due to (7) and thus the trajectory is continuous. However, switching from $q_a > 0$ (i.e. FF^{II} and FB^{II} are active) to FF^I and FB^I at time $t = t_s$ when $q_a = 0$, the desired swash plate angle $\varphi_{p,d}$ has to satisfy the following relations at $t = t_s$

$$\varphi_{p,d} = \frac{1}{k_p} \left(\frac{V_l}{\beta} \dot{p}_{l,d} + \hat{k}_l \sqrt{p_{l,d}} + q_{a,d} \right) \quad (15)$$

²Note that the actual design of the feedback controllers will be performed in the next subsection.

according to (11) for FF^{II} and

$$\varphi_{p,d} = \frac{1}{k_p} \left(\frac{V_l}{\beta} \dot{p}_{l,d} + \hat{k}_l \sqrt{p_{l,d}} \right) \quad (16)$$

according to (7) for FF^I . Of course there is no reason for $q_{a,d}$ to be zero at time $t = t_s$, since the switching condition $q_a(t_s) = 0$ only leads to $q_{a,d}(t_s) = -q_{a,c}(t_s)$. Consequently, switching at $q_a = 0$ in general provokes a discontinuous time evolution of $\varphi_{p,d}$ and thus of e_φ . Note that this behavior originates from the fact that the relative degree of the output to be controlled p_l is changing when switching between the systems Σ^I and Σ^{II} due to (4) and (5), respectively. See, e.g., Isidori (2001) for more details on the notion of relative degree of a nonlinear system.

There is, however, a second problem which occurs in connection with a switching based on the condition $q_a = 0$. If $FF^I + FB^I$ yields $q_a = 0$ this does not necessarily imply that $FF^{II} + FB^{II}$ also yields $q_a = 0$. In order to clarify this, let us consider the situation where $q_a < 0$ with FF^I and FB^I active and switching takes place if q_a from $FF^I + FB^I$ crosses zero, i.e. $q_a = 0$. In this case, q_a calculated from $FF^{II} + FB^{II}$ may also be negative which would cause immediate switching back to FF^I and FB^I . Thus, there is a set where neither FF^I and FB^I nor FF^{II} and FB^{II} are valid. As a result (and for perfect switching), a sliding motion along the (sliding) submanifold $q_a = 0$ of $FF^I + FB^I$ would take place.

The first problem, i.e. the discontinuity of the desired trajectories, can be solved by switching the feedforward control FF^I and FF^{II} and the feedback control FB^I and FB^{II} independently. Therefore, the zero crossing of the desired volume flow $q_{a,d}$ is used as a switching criterion for the feedforward control instead of the actuator volume flow q_a . Since $q_{a,d} = 0$ yields the same $\varphi_{p,d}$ for FF^I and FF^{II} , cf. (15) and (16), this switching criterion avoids the aforementioned problems when switching from FF^{II} to FF^I .

The sliding motion of the controller can also be circumvented by switching the feedback control FB^I and FB^{II} independently of the system. In contrast to the feedforward control the choice of a suitable switching criterion is much more complicated in this case since the feedback control may consist of arbitrary nonlinear functions of the states e_p and e_φ . Furthermore, the independent switching of the feedforward and the feedback control requires the proof of the stability of the closed-loop system of all eight possible combinations of feedforward control (FF^I , FF^{II}), feedback control (FB^I , FB^{II}) and systems (Σ^I , Σ^{II}) with one common Lyapunov function. In order to simplify matters, in this work a common feedback law $FB^I = FB^{II}$ will be used.

The general procedure of the feedback controller design is as follows: First, a feedback controller and a control Lyapunov function are designed for the error system (13), resulting from the application of FF^I to Σ^I . Afterwards, the stability of the closed-loop system for the other three combinations of feedforward control and system (FF^{II} , Σ^{II}), (FF^I , Σ^{II}) and (FF^{II} , Σ^I), respectively, is proven using a common Lyapunov function and feedback law. This, of course, implies the stability of the overall switched closed-loop control system.

Feedforward FF^I with System Σ^I

Applying FF^I to Σ^I results in the error system (13). For the design of the feedback controller it is assumed that the estimated value \hat{k}_l is exactly equal to the real value k_l (certainty equivalence condition, see, e.g., Krstić, Kanellakopoulos & Kokotović (1995)). The design of an estimator for k_l and the proof of the stability of the overall closed-loop system comprising the feedforward control, the feedback control and the estimator will be given in the next section.

As a starting point the positive definite function W_c

$$W_c = \frac{1}{2} \delta_1 e_p^2 + \frac{1}{2} \delta_2 e_\varphi^2, \quad (17)$$

with positive constants $\delta_1, \delta_2 > 0$, is chosen as a possible candidate for a control Lyapunov function (CLF). The change of W_c along a solution of the error system (13) reads as

$$\begin{aligned} \frac{d}{dt} W_c = & -\frac{\delta_1 \beta k_l}{V_l} \left(\sqrt{e_p + p_{l,d}} - \sqrt{p_{l,d}} \right) e_p \\ & + \frac{\delta_1 \beta k_p}{V_l} e_p e_\varphi - \frac{\delta_2}{A_a r_a} e_\varphi q_{a,c}. \end{aligned} \quad (18)$$

For the considered application a simple feedback control law of the form

$$q_{a,c} = \lambda_p e_p + \lambda_\varphi e_\varphi \quad (19)$$

with constant controller parameters $\lambda_p, \lambda_\varphi > 0$, is chosen. At this point one may wonder why a linear feedback controller suffices in terms of the demands on the closed-loop dynamics. Note that the excellent performance of the overall closed-loop system (cf. Section 5) is mainly due to (i) the feedforward controller, which systematically accounts for the nonlinearities in the tracking case and (ii) the nonlinear load estimator for k_l , to be designed in the next section, in the disturbance case in combination with (iii) the proposed switching strategy.

Substituting the feedback control law (19) into (18) and setting δ_1 to

$$\delta_1 = \frac{\delta_2 V_l}{A_a r_a k_p \beta} \lambda_p \quad (20)$$

results in

$$\frac{d}{dt} W_c = -\frac{\delta_2 \lambda_p k_l}{A_a r_a k_p} \left(\sqrt{e_p + p_{l,d}} - \sqrt{p_{l,d}} \right) e_p - \frac{\delta_2 \lambda_\varphi}{A_a r_a} e_\varphi^2. \quad (21)$$

Clearly, since $k_p, k_l > 0$ the right-hand side of (21) is negative definite and this proves the asymptotic stability of the closed-loop system (13), i.e. FF^I with Σ^I , and (19).

Similar results can be obtained for the three other combinations of feedforward control and system (FF^{II} , Σ^{II}), (FF^I , Σ^{II}) and (FF^{II} , Σ^I), see the Appendix A. Thus, the stability of the closed-loop system consisting of the switched feedforward control, the common feedback control and the switched system is proven if the certainty equivalence condition $k_l = \hat{k}_l$ holds. In the next section an estimation of \hat{k}_l will be derived and the stability of the overall closed-loop system will be proven.

4. Estimation of the load coefficient k_l

The design of the estimator for the load coefficient k_l is based on the assumption that k_l is unknown but constant. In this contribution, two different estimators will be derived. The first rather simple approach is straightforward and well known from literature but has the drawback that it can hardly be tuned to meet the demands on the dynamic performance and on the robustness. In particular these deficiencies become apparent when applying this simple estimator to the experimental setup. For this reason, an extended estimator also will be presented where the whole measurement information is exploited within the design process.

4.1. Simple estimator

The simple estimator is supposed to take the form

$$\frac{d}{dt}\hat{k}_l = -\chi_k(e_p, e_\varphi, t), \quad (22)$$

where the right-hand side χ_k of (22) has to be determined. In order to do so, the CLF (17) is extended by a quadratic term in the estimation error $\hat{e}_k = k_l - \hat{k}_l$

$$W_{tot} = W_c + W_e = \frac{1}{2}\delta_1 e_p^2 + \frac{1}{2}\delta_2 e_\varphi^2 + \frac{1}{2}\frac{1}{\lambda_k}\hat{e}_k^2, \quad (23)$$

with the tuning parameter $\lambda_k > 0$ of the estimator. Before calculating the change of W_{tot} along a solution of the error system (13), (14), (42) or (47), respectively, it is useful to rewrite the right-hand sides in such a way that only expressions with k_l and $k_l - \hat{k}_l = \hat{e}_k$ do appear but no ones which are explicitly weighted with \hat{k}_l . Note that this can always be achieved since the right-hand sides of the error systems (13), (14), (42) and (47) are all affine in the load coefficient k_l . For the error system (13) this rearrangement of the right-hand side exemplarily yields

$$\frac{d}{dt}e_\varphi = -\frac{1}{A_a r_a}q_{a,c} \quad (24a)$$

$$\begin{aligned} \frac{d}{dt}e_p = & \frac{\beta}{V_l} \left(k_p e_\varphi - k_l \sqrt{e_p + p_{l,d}} + k_l \sqrt{p_{l,d}} \right) \\ & - \underbrace{\frac{\beta}{V_l} (k_l - \hat{k}_l)}_{\hat{e}_k} \sqrt{p_{l,d}}. \end{aligned} \quad (24b)$$

Analogously, all other error systems can be rewritten to exhibit a similar structure. The first term of (24b) equals the error system (13) if the certainty equivalence condition holds and the second term of (24b) accounts for the estimation error.

Now, the change of the overall Lyapunov function W_{tot} along a trajectory of the closed-loop system (24) with (19) and (22) can be calculated as

$$\begin{aligned} \frac{d}{dt}W_c = & -\frac{\delta_2 k_l \lambda_p}{A_a r_a k_p} \left(\sqrt{e_p + p_{l,d}} - \sqrt{p_{l,d}} \right) e_p - \frac{\delta_2 \lambda_\varphi}{A_a r_a} e_\varphi^2 \\ & - \frac{\delta_2 \lambda_p}{A_a r_a k_p} \sqrt{p_{l,d}} e_p \hat{e}_k + \frac{1}{\lambda_k} \hat{e}_k \chi_k. \end{aligned} \quad (25)$$

This result corresponds to (21) except for the last two terms. In order to render \dot{W}_{tot} negative semi-definite, the third term in

(25) is cancelled out by the last term. Thus, the estimator due to (22) reads as

$$\frac{d}{dt}\hat{k}_l = -\hat{\lambda}_k \frac{\delta_2 \lambda_p}{A_a r_a k_p} \sqrt{p_{l,d}} e_p \quad (26)$$

Obviously, using the same approach for the other three error systems yields the same result. Since the calculations are straightforward they are omitted here. With this, the stability of the closed-loop system comprising the switched feedforward control, the common feedback control, the estimator and the switched system has been proven.

Simulation studies and experimental results with the simple estimator, however, show that (i) a suitable choice of $\hat{\lambda}_k$ is very difficult to find and that (ii) the demands on the dynamic performance and accuracy cannot be achieved. Furthermore, the estimator shows a weak robustness to model uncertainties. Therefore, the simple estimator is not feasible for practical implementation.

4.2. Extended estimator

The basic idea in the development of the extended estimator for the load coefficient k_l is to additionally estimate the load pressure p_l , although this quantity is available by measurement. The main reason for this is to provide additional degrees-of-freedom for the design and parametrization of the estimator.

The estimator for the load pressure p_l is composed of a prediction and a correction part, where the predictor is basically a copy of the mathematical model (4b), (5b) and the corrector term $\chi_p(e_p, e_\varphi, t)$ is used to stabilize and adjust the estimator dynamics, namely

$$\frac{d}{dt}\hat{p}_l = \frac{\beta}{V_l} \left(k_p e_\varphi - \hat{k}_l \sqrt{\hat{p}_l} \right) - \chi_p, \quad \text{for } q_a \leq 0 \quad (27a)$$

$$\frac{d}{dt}\hat{p}_l = \frac{\beta}{V_l} \left(k_p e_\varphi - \hat{k}_l \sqrt{\hat{p}_l - q_a} \right) - \chi_p, \quad \text{for } q_a > 0. \quad (27b)$$

As it can be seen the switching between (27a) and (27b) relies on the zero-crossing of the actuator volume flow q_a . Thus, the estimator (27) is switched synchronously to the system (4), (5). For the estimation of the load coefficient k_l the same approach as in (22) is used

$$\frac{d}{dt}\hat{k}_l = -\chi_k(e_p, e_\varphi, t). \quad (28)$$

Introducing the estimation errors $\hat{e}_p = p_l - \hat{p}_l$ and $\hat{e}_k = k_l - \hat{k}_l$ it can be easily seen that the error system for both systems Σ^I and Σ^{II} has the identical form

$$\frac{d}{dt}\hat{e}_p = -\frac{\beta}{V_l} \sqrt{\hat{p}_l} \hat{e}_k + \chi_p(e_p, e_\varphi, t) \quad (29a)$$

$$\frac{d}{dt}\hat{e}_k = \chi_k(e_p, e_\varphi, t). \quad (29b)$$

The corrector terms $\chi_p(e_p, e_\varphi, t)$ and $\chi_k(e_p, e_\varphi, t)$ in (29) have to be designed in order to allow for a proof of the stability of the overall closed-loop system comprising the feedforward and the feedback controller, the system and the extended estimator.

However, before proving the stability of the overall closed-loop system, the stability of the extended estimator itself will be analyzed. For this purpose the Lyapunov function candidate

$$W_e = \frac{1}{2} \hat{e}_p^2 + \frac{1}{2} \frac{1}{\hat{\lambda}_k} \hat{e}_k^2 \quad (30)$$

with the estimator parameter $\hat{\lambda}_k > 0$ is chosen. The change of W_e along a solution of (29) is then given by

$$\frac{d}{dt} W_e = -\frac{\beta}{V_l} \sqrt{p_l} \hat{e}_p \hat{e}_k + \hat{e}_p \chi_p + \frac{1}{\hat{\lambda}_k} \hat{e}_k \chi_k. \quad (31)$$

In order to compensate for the first indefinite term, χ_k is fixed as

$$\chi_k(e_p, e_\varphi, t) = \hat{\lambda}_k \frac{\beta}{V_l} \sqrt{p_l} \hat{e}_p. \quad (32)$$

Then, the choice of the corrector term χ_p in the form

$$\chi_p(e_p, e_\varphi, t) = -\hat{\lambda}_p \hat{e}_p \quad (33)$$

with the estimation parameter $\hat{\lambda}_p > 0$ renders \dot{W}_e in (31) negative semi-definite. This implies stability in the sense of Lyapunov of the extended estimator.

Up to now, the estimator has been analyzed separately from the rest of the system. In order to study the stability of the overall closed-loop system with the extended estimator the overall Lyapunov function, cf. (17) and (30)

$$W_{tot} = W_c + W_e = \frac{1}{2} \delta_1 e_p^2 + \frac{1}{2} \delta_2 e_\varphi^2 + \frac{1}{2} \hat{e}_p^2 + \frac{1}{2} \frac{1}{\hat{\lambda}_k} \hat{e}_k^2 \quad (34)$$

is used. Keeping the analysis of the simple estimator, especially (24), (25) and (26), in mind, it can be seen that the time derivative \dot{W}_{tot} along a solution of the overall closed-loop system is negative except for the term

$$-\frac{\delta_2 \lambda_p}{A_a r_a k_p} \sqrt{p_{l,d}} e_p \hat{e}_k. \quad (35)$$

This term can be cancelled out by augmenting $\chi_k(e_p, e_\varphi, t)$ from (32) in the form

$$\chi_k = \hat{\lambda}_k \left(\frac{\beta}{V_l} \sqrt{p_l} \hat{e}_p + \frac{\delta_2 \lambda_p}{A_a r_a k_p} \sqrt{p_{l,d}} e_p \right). \quad (36)$$

Summarizing, the extended estimator reads as

$$\frac{d}{dt} \hat{p}_l = \frac{\beta}{V_l} (k_p \varphi_p - \hat{k}_l \sqrt{p_l}) + \hat{\lambda}_p \hat{e}_p \quad (37a)$$

$$\frac{d}{dt} \hat{k}_l = -\hat{\lambda}_k \left(\frac{\beta}{V_l} \sqrt{p_l} \hat{e}_p + \frac{\delta_2 \lambda_p}{A_a r_a k_p} \sqrt{p_{l,d}} e_p \right) \quad (37b)$$

for $q_a \leq 0$ and

$$\frac{d}{dt} \hat{p}_l = \frac{\beta}{V_l} (k_p \varphi_p - \hat{k}_l \sqrt{p_l} - q_a) + \hat{\lambda}_p \hat{e}_p \quad (38a)$$

$$\frac{d}{dt} \hat{k}_l = -\hat{\lambda}_k \left(\frac{\beta}{V_l} \sqrt{p_l} \hat{e}_p + \frac{\delta_2 \lambda_p}{A_a r_a k_p} \sqrt{p_{l,d}} e_p \right) \quad (38b)$$

for $q_a > 0$.

5. Measurement Results

In this section, the properties of the proposed control strategy comprising the feedforward controller FF^I (7), (9) and FF^{II} (11) and (12), the common feedback controller (19) and the extended estimator (37) and (38), are analyzed by means of measurement results of a test stand. The test stand was designed and built by the company HYDAC Electronic GmbH, see Fig. 3. The main components of this test stand are the variable displacement axial piston pump driven by an induction machine and controlled by the control valve, the load volume and the load orifice. The schematic diagram of the hydraulic circuit of the test stand is given in Fig. 2 and the parameters of the system are summarized in Table 1.

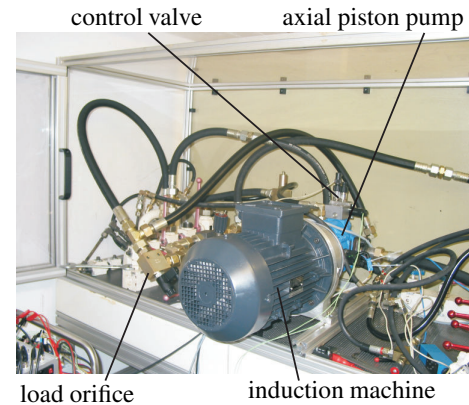


Figure 3: Experimental setup of the test stand for the axial piston pump.

| parameter | symbol | value | unit |
|---------------------------|-------------------|----------------------|---------------------------|
| bulk modulus | β | $1.6 \cdot 10^9$ | Pa |
| eff. area of actuator | A_a | 300 | mm ² |
| eff. radius of actuator | r_a | 50 | mm |
| number of pistons | n_p | 9 | |
| area of piston | A_p | 165 | mm ² |
| radius of rot. of pistons | r_p | 30 | mm |
| angular vel. of pump | ω_p | 50π | $\frac{1}{s}$ |
| pump coefficient | k_p | $2.23 \cdot 10^{-3}$ | $\frac{m^3}{s}$ |
| min. swash plate angle | $\varphi_{p,min}$ | -1.5 | ° |
| max. swash plate angle | $\varphi_{p,max}$ | 18 | ° |
| load volume | V_l | 1.5 | l |
| min. load coeff. | $k_{l,min}$ | $10 \cdot 10^{-9}$ | $\frac{m^3}{s \sqrt{Pa}}$ |
| nom. load coeff. | $k_{l,nom}$ | $90 \cdot 10^{-9}$ | $\frac{m^3}{s \sqrt{Pa}}$ |
| max. load coeff. | $k_{l,max}$ | $140 \cdot 10^{-9}$ | $\frac{m^3}{s \sqrt{Pa}}$ |

Table 1: Parameters of the pump and the load.

The actuator for tilting the swash plate is controlled by a (3/3) proportional directional valve, cf. Fig. 2. In contrast to the previous assumption, the volume flow q_a into the actuator cannot be directly assigned by means of this valve. In fact, only the position s_v of the spool of the valve can be controlled directly.

The volume flow q_a is given in the form

$$q_a = \alpha \sqrt{\frac{2}{\rho}} \left(A_{la}(s_v) \sqrt{p_l - p_a} - A_{at}(s_v) \sqrt{p_a - p_t} \right), \quad (39)$$

where α denotes the constant discharge coefficient, ρ is the mass density of the oil and $A_{la}(s_v)$ and $A_{at}(s_v)$ are the opening areas of the valve from the load to the actuator and from the actuator to the tank, respectively. Furthermore, p_l is the load pressure, p_a denotes the actuator pressure and $p_t = 0$ is the tank pressure. In the system under consideration a valve with a small negative overlap is used, whose opening characteristics are depicted in Fig. 4.

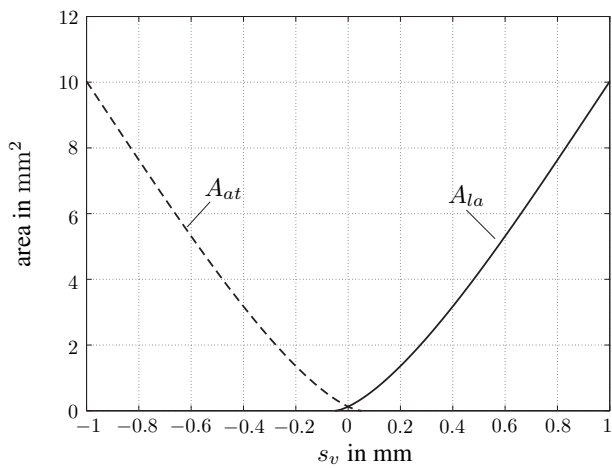


Figure 4: Opening characteristics $A_{la}(s_v)$ and $A_{at}(s_v)$ of the proportional valve.

In order to calculate the real control input, i.e. the valve spool position s_v , from the virtual control input q_a , (39) is solved for s_v . A unique solution of this equation always exists, although it can only be evaluated numerically. With this it is possible to compensate for the nonlinearities of the valve (servo-compensation) such that the spool position s_v can be calculated from the volume flow q_a . Thereby, as already mentioned before, the dynamics of the valve is neglected since it is considerably faster (rise time of approximately 5 ms) than the dynamics of the system.

The control strategy, extended by the servo-compensation, was realized in form of a SIMULINK C-code s-function, compiled using MATLAB REAL-TIME WORKSHOP and implemented on a dSPACE realtime hardware DS1103. Thereby, a sampling time of $T_s = 1$ ms is used. Furthermore, the parameters of the controller and the estimator are chosen according to Table 2.

In the first measurement result the tracking behavior of the load pressure p_l is analyzed. Therefore, two measurements are performed, one with a small load coefficient $k_l = k_{l,min}$ (see the left-hand side of Fig. 5) and one with a larger, nominal load coefficient $k_l = k_{l,nom}$ (see the right-hand side of Fig. 5). As can be seen from the time-evolution of the load pressure p_l an excellent tracking performance is achieved independent of the actual value of the load coefficient. On the other hand, the different

| parameter | value |
|-------------------|----------------------|
| λ_p | $8 \cdot 10^{-11}$ |
| λ_φ | $5 \cdot 10^{-3}$ |
| $\hat{\lambda}_p$ | 600 |
| $\hat{\lambda}_k$ | $5 \cdot 10^{-27}$ |
| δ_2 | $1.5 \cdot 10^{-14}$ |

Table 2: Parameters of the controller and extended estimator.

load coefficients have a large influence on the trajectories of the swash plate angle φ_p . Obviously, this is due to the fact that only a small volume flow q_p of the pump is necessary to provide the (small) load volume flow $q_l = k_{l,min} \sqrt{p_l}$ for the small load coefficient while a much higher volume flow q_p is necessary for the larger load coefficient $k_{l,nom}$. The influence of the different load coefficients can also be seen in the plots of the actuator volume flow q_a and the real control input s_v , which are given at the bottom of Fig. 5.

The second measurement result, given in Fig. 6, shows the behavior of the system for rapid changes of the load coefficient. Here, the load orifice is closed and opened as fast as possible while a desired trajectory $p_{l,d}(t)$ in the load pressure is tracked. Of course, the fast change of k_l yields to significant errors in the load pressure but these errors are compensated in a very fast way. At this point it is worth mentioning that the stability proof of the overall closed-loop system, cf. Section 4.2, relies on the assumption that the load coefficient is unknown but constant. Clearly, the case of rapidly changing loads is not covered by the stability proof but the measurement results show that the control strategy is reliable also in this situation. The dynamical behavior of the estimation of the load coefficient, as given on the right-hand side of Fig. 6, shows that the estimation \hat{k}_l tracks the rapidly changing load coefficient in an excellent manner. Thereby, it has to be mentioned that the rather large overshoot in the estimation of the load coefficient can be reduced by adjusting the parameters of the estimator. However, the main focus of the control strategy is good tracking of the load pressure p_l and not the exact estimation of the load coefficient. For this task, the chosen parameters of the controller and estimator have proven to be feasible in practical application and turned out to be a good compromise between tracking performance of the load pressure and a good estimation of the load coefficient.

In the final measurement result, the tracking behavior of the load pressure is analyzed for slowly varying load coefficients. Here, the load coefficient k_l is slowly increased while the load pressure should track a rectangular like reference trajectory, cf. Fig. 7. For this case again an excellent tracking performance can be achieved, while at the same time a good estimation of the load coefficient is obtained.

To sum it up, the measurement results show a very good performance of the overall control strategy and thus prove the practical feasibility of the proposed control strategy comprising the feedforward control, the feedback control and the extended estimator.

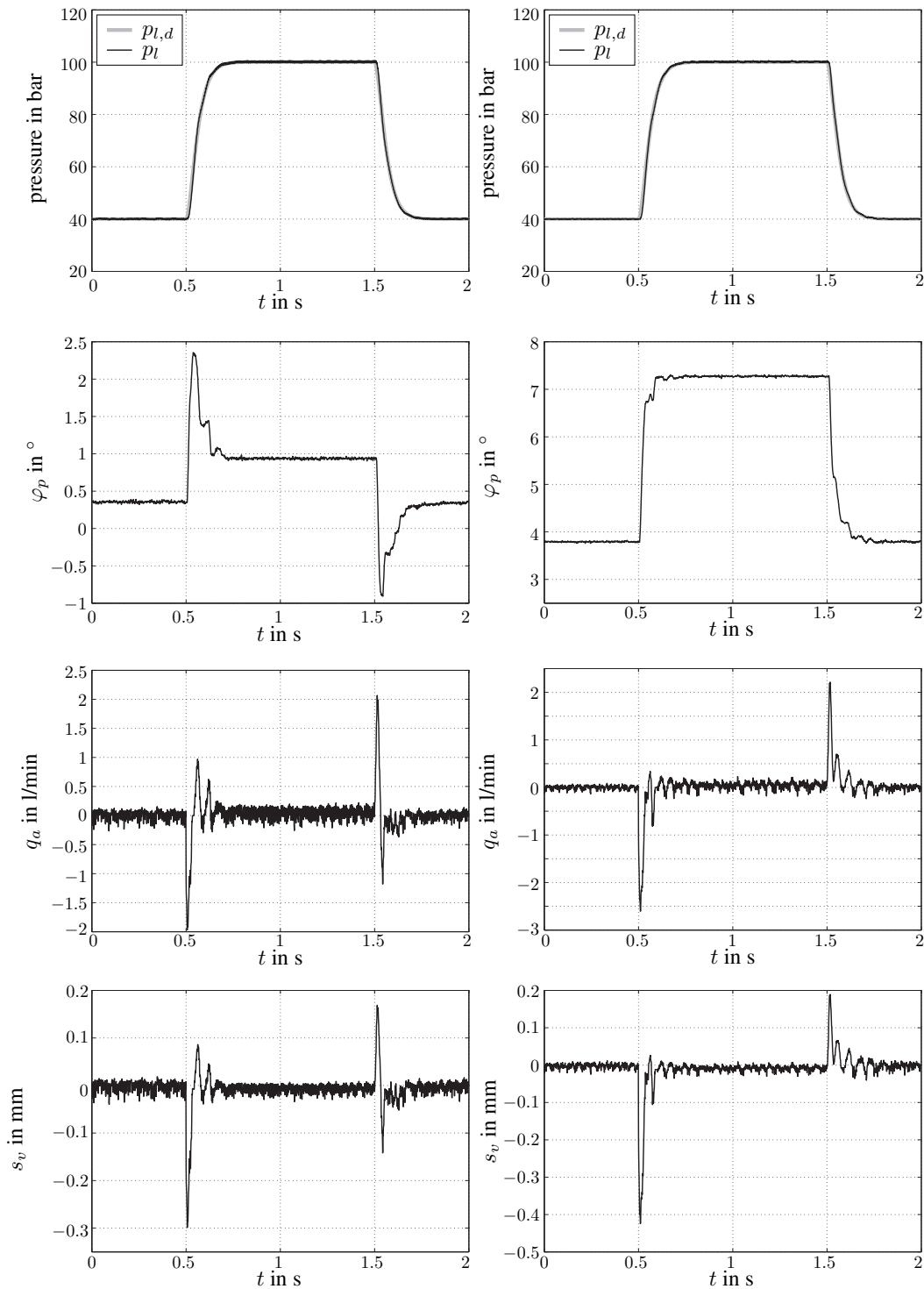


Figure 5: Measurement results for the tracking behavior of the load pressure p_l for a small load coefficient $k_l = k_{l,min}$ on the left-hand side and a larger, nominal load coefficient $k_l = k_{l,nom}$ on the right-hand side.

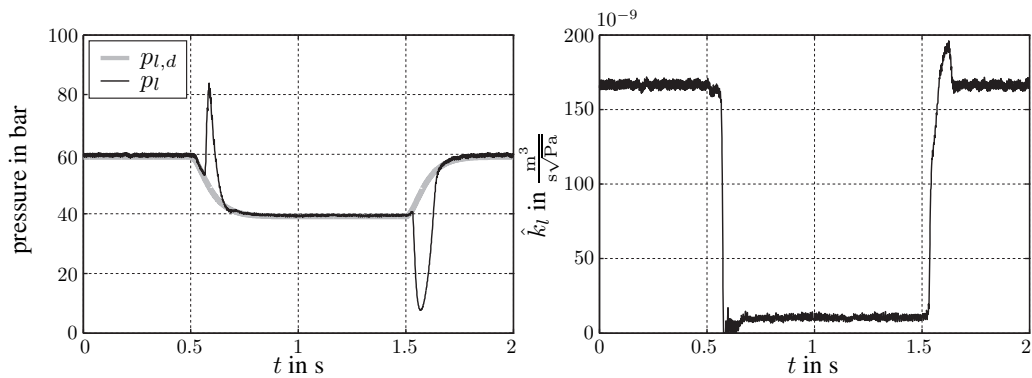


Figure 6: Measurement results for a rapid change of the load coefficient k_l while tracking a trajectory in the load pressure p_l .

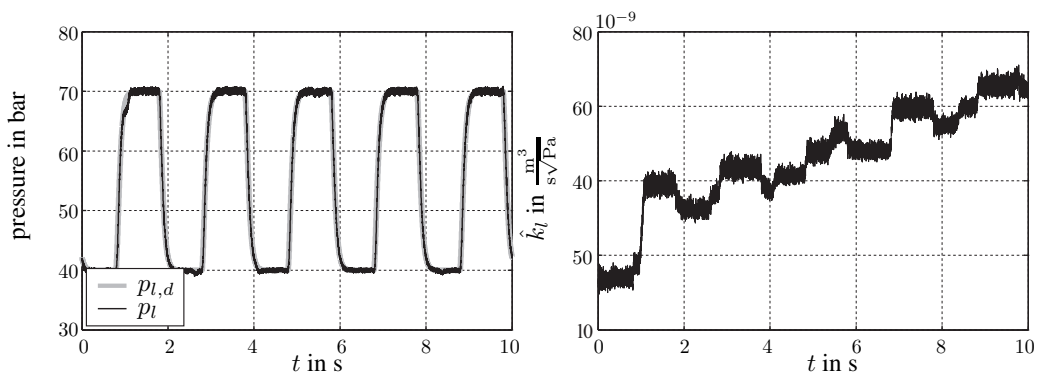


Figure 7: Measurement results for the slow change of the load coefficient k_l while tracking a trajectory in the load pressure p_l .

6. Conclusion

In this work a new (nonlinear) control concept for the pressure control of self-supplied variable displacement axial piston pumps with variable load was designed. First, the basic setup of the electrohydraulic system and its mathematical model was described. Therein it was pointed out that the switching character of the mathematical model, which is due to the self-supply mechanism of the pump, and the fast changing unknown loads constitute the main challenges for the controller design. In order to solve this control task, a two degrees-of-freedom control structure comprising a feedforward and a feedback controller in combination with a load estimator was proposed. The advantages of this approach are (i) the systematic proof of the closed-loop stability for unknown but constant load coefficients based on Lyapunov’s stability theory, (ii) the model-based design, which allows an easy implementation of the control concept to other installation sizes in the same model range, and (iii) the simple parameterization by means of a few controller parameters. The feasibility of the control strategy was shown by measurement results, whereby an excellent robustness behavior and a superior tracking performance could be achieved. Furthermore, the practical use of the proposed control concept is affirmed by the industrial partner who also stresses the significant improvement of the proposed control concept compared to

the existing industrial solution.

A. Proof of stability

A.1. Feedforward FF^{II} with System Σ^{II}

The error system for the feedforward controller FF^{II} applied to the system Σ^{II} is given in (14). By using the certainty equivalence condition, the CLF from (17) and the feedback control (19) with (20) yields the change of the CLF W_c along the solution of (14)

$$\begin{aligned} \frac{d}{dt} W_c = & -\frac{\delta_2 k_l \lambda_p}{A_a r_a k_p} \left(\sqrt{e_p + p_{l,d}} - \sqrt{p_{l,d}} \right) e_p \\ & - \frac{\delta_2}{A_a r_a} \left(\frac{\lambda_p^2}{k_p} e_p^2 + \frac{\lambda_p \lambda_\varphi}{k_p} e_p e_\varphi + \lambda_\varphi e_\varphi^2 \right). \end{aligned} \quad (40)$$

The right-hand side of (40) is negative definite if the condition

$$4k_p > \lambda_\varphi > 0 \quad (41)$$

is fulfilled, which also implies the asymptotic stability of the closed-loop system (14), (19).

A.2. Feedforward FF^I with System Σ^{II}

Due to the independent switching of the feedforward part and the system it may happen that the feedforward control FF^I is applied to the system Σ^{II} and vice versa FF^{II} is applied to Σ^I . Using FF^I in combination with Σ^{II} results in the error system

$$\frac{d}{dt}e_\varphi = -\frac{1}{A_a r_a} q_{a,c} \quad (42a)$$

$$\frac{d}{dt}e_p = \frac{\beta}{V_l} (k_p e_\varphi - k_l \sqrt{e_p + p_{l,d}} + \hat{k}_l \sqrt{p_{l,d}} - q_a). \quad (42b)$$

Inserting the control law (19) into (42) and presuming the certainty equivalence condition, the change of the CLF W_c along a solution of the error system (42) reads as

$$\begin{aligned} \frac{d}{dt}W_c = & -\frac{\delta_2 k_l \lambda_p}{A_a r_a k_p} (\sqrt{e_p + p_{l,d}} - \sqrt{p_{l,d}}) e_p \\ & -\frac{\delta_2 \lambda_\varphi}{A_a r_a} e_\varphi^2 - \frac{\delta_2 \lambda_p}{A_a r_a k_p} e_p q_a. \end{aligned} \quad (43)$$

This result equals (21) except for the last indefinite term

$$-\frac{\delta_2 \lambda_p}{A_a r_a k_p} e_p q_a. \quad (44)$$

Since the actuator volume flow q_a is positive for the system Σ^{II} , the indefinite term (44) is negative for $e_p > 0$. Thus, \dot{W}_c is negative definite for $e_p > 0$. In order to show a similar relation for $e_p < 0$, the quantity q_a is replaced by $q_a = q_{a,d} + q_{a,c}$ in (43), with $q_{a,c}$ according to (19). Doing so, (43) can be rewritten in the form

$$\begin{aligned} \frac{d}{dt}W_c = & -\frac{\delta_2 k_l \lambda_p}{A_a r_a k_p} (\sqrt{e_p + p_{l,d}} - \sqrt{p_{l,d}}) e_p - \frac{\delta_2}{A_a r_a} \\ & \left(\frac{\lambda_p^2}{k_p} e_p^2 + \frac{\lambda_p \lambda_\varphi}{k_p} e_p e_\varphi + \lambda_\varphi e_\varphi^2 \right) - \frac{\delta_2 \lambda_p}{A_a r_a k_p} e_p q_{a,d}, \end{aligned} \quad (45)$$

which corresponds to (40) except for the last indefinite term

$$-\frac{\delta_2 \lambda_p}{A_a r_a k_p} e_p q_{a,d}. \quad (46)$$

Now, since FF^I is only active if $q_{a,d}$ is negative, the expression (46) is negative for $e_p < 0$ which also proves the negative definiteness of \dot{W}_c for $e_p < 0$, provided that (41) holds. Summarizing, it has been shown that \dot{W}_c is negative definite and thus the stability of the closed-loop system (42), where FF^I is applied to Σ^{II} , with the control law (19) subject to the inequality (41) is proven.

A.3. Feedforward FF^{II} with System Σ^I

The last case to be considered is the feedforward controller FF^{II} applied to the system Σ^I . In this case the error system reads as

$$\frac{d}{dt}e_\varphi = -\frac{1}{A_a r_a} q_{a,c} \quad (47a)$$

$$\frac{d}{dt}e_p = \frac{\beta}{V_l} (k_p e_\varphi - k_l \sqrt{e_p + p_{l,d}} + \hat{k}_l \sqrt{p_{l,d}} + q_{a,d}). \quad (47b)$$

Similar arguments as in the previous subsection show that also in this case the change of the common Lyapunov function (17) along a solution of (47) is negative definite for $\lambda_p > 0$ and λ_φ satisfying the inequality condition (41).

References

- Blackburn J.F., Reethof G. & Shearer J.L. (1960). *Fluid Power Control*. New York: John Wiley & Sons.
- Branicky M.S. (1995) *Studies in hybrid systems: Modeling, analysis and control*. PhD Thesis Massachusetts Institute of Technology.
- Branicky M.S. (1998) Multiple Lyapunov functions and other analysis tools for switched and hybrid systems. *IEEE Trans. on Automatic Control*, 43(4), 475-482.
- DeCarlo R.A., Branicky M.S., Pettersson S. & Lennartson B. (2000). Perspectives and results on stability and stabilizability of hybrid systems. *Proc. of the IEEE*, 88(7), 1069-1082.
- Frieden F. (2006) *Oil-Hydraulics (in German)*. Berlin, Germany: Springer.
- Fliess M., Lévine J., Martin P. & Rouchon P. (1995) Flatness and Defect of Non-linear Systems: Introductory Theory and Examples. *International J. of Control*, 61(6), 1327-1361.
- Fuchshumer F. (2009) *Modeling, analysis and nonlinear model-based control of variable displacement axial piston pumps (in German)*. PhD Thesis Vienna University of Technology.
- Grabbel J. & Ivantysynova M. (2005) An investigation of swash plate control concepts for displacement controlled actuators. *Int. Journal of Fluid Power*, 6(2), 19-36.
- Ivantysyn J. & Ivantysynova M. (1993) *Hydrostatic pumps and drives (in German)*. Würzburg, Germany: Vogel.
- Isidori A. (2001) *Nonlinear Control Systems*. London, UK: Springer.
- Khalil H.K. (2002) *Nonlinear Systems, 3rd Ed.* Upper Saddle River: Prentice Hall.
- Krstić M., Kanellakopoulos I. & Kokotović P. (1995) *Nonlinear and Adaptive Control Design*. New York: John Wiley & Sons.
- Liberzon D. (2003) *Switching in Systems and Control*. Boston, USA: Birkhäuser.
- Manring N.D. & Johnson R.E. (1996) Modeling and designing a variable-displacement open-loop pump. *ASME J. of Dynamic Systems, Measurement and Control*, 118(2), 267-271.
- Manring N.D. (2005) *Hydraulic Control Systems*. New Jersey, USA: John Wiley & Sons.
- McCloy D. & Martin H.R. (1980) *Control of Fluid Power: Analysis and Design*. New York: John Wiley & Sons.
- Merritt H.E. (1967) *Hydraulic Control Systems*. New York: John Wiley & Sons.
- Wu D., Burton R., Schoenau G. & Bitner D. (2002) Establishing operating points for a linearized model of a load sensing system. *Int. Journal of Fluid Power*, 3(2), 47-54.